7452

J. Am. Chem. Soc. **1992**, *114*, 7452–7458

Density Functional Study of CO Chemisorption on Model Clusters of Rh and Pd: A Comparative Analysis of the Site Selection

A. Goursot,*,† I. Papai,‡,§ and D. R. Salahub‡

Contribution from the URA 418 CNRS, Ecole de Chimie, 8 rue de l'Ecole Normale, 34053 Montpellier, Cédex 1, France, and Département de Chimie, Université de Montréal, CP 6128, Succ. A, Montréal, Québec, Canada. Received February 10, 1992

Abstract: Density functional calculations have been performed for the Rh_2 and Pd_2 dimers and for Rh_4 and Pd_4 clusters, in order to compare the Rh–Rh and Pd–Pd bonds. Using the Rh_4 and Pd_4 clusters as models for (111) surfaces, chemisorption of CO at top, bridge, and 3-fold sites has also been studied. The calculated optimized geometries and normal frequencies for the adsorbed CO are reported, and the trends are compared with experimental results on Rh and Pd surfaces. Chemisorption energies as well as electronic properties of the Rh_4CO and Pd_4CO models are compared for the three sites. The gradient corrected binding energies of CO are clearly different for the three sites of Pd clusters, the largest corresponding to the 3-fold site adsorption. In contrast, these energies are rather similar for the three sites of the Rh clusters. Analysis of the Mulliken gross atomic populations shows that the atomic configuration of the metal atom(s) bonded to CO is a characteristic of the adsorption site. These results are rationalized by assuming that the metal atom(s) of the surface, to which CO is bonded, has some "memory" of the energetic properties of the isolated Rh or Pd atom, which governs its ability to adopt a specific configuration and hence its bonding capability.

I. Introduction

Rh and Pd catalysts have been extensively investigated for CO + H_2 conversion reactions.[1,2] The hydrogenation of carbon monoxide on supported Rh particles produces a variety of compounds such as hydrocarbons, alcohols, aldehydes, and acids. Both activity and selectivity of Rh catalysts can be drastically altered by changing their dispersion,[3] and it has been suggested that these differences in catalytic properties are caused by differences in the morphology of the particles.[4] Pd is more active than Rh for the production of methanol, and it has been proposed that the intermediate in the Fischer–Tropsch synthesis is a surface carbide, produced by the dissociative adsorption of CO. Carbon monoxide has been used for a long time as a probe for surface characterizations. Among other things, its vibrational properties reflect the metal–CO bond strength at the various possible sites and also the influence of the direct environment. At similar coverages, the adsorption sites on Rh and Pd are different, and also the ordering of the CO overlayer is different. On Pd catalysts, CO mainly adsorbs at multibonded sites, whereas linear (on-top) adsorption and production of *gem*-dicarbonyl species are reported for Rh catalysts. It is thus a challenge, not only for theoretical chemistry but also for surface science and catalysis, to understand why CO chemisorption is different on these two metals.

In fact, metal–CO bonding has been extensively studied by a great variety of theoretical approaches, in particular for Ni, Cu, Pd, and Pt. However, only a few studies have compared different metals and/or different sites.[5–13] The interaction between CO and a metal atom was first described by Blyholder, in a model based on Hückel molecular orbitals (MOs), involving a 5σ CO donation to the metal, associated with a backdonation to the empty $2\pi^*$ CO orbital.[14] This description is compatible with photoelectron spectroscopy experiments of CO chemisorbed on different metal surfaces.[15–20] Indeed, a typical feature of CO chemisorption is represented by the stabilization of 5σ, so that the ionization potentials of 5σ and 1π become superposed. This energy shift of 5σ can be considered as an indication that this orbital participates in the metal–CO bonding, although it has also been related to geometric features of the adsorbed CO molecule.[21] Inverse photoemission studies have attempted to establish the role of the $2\pi^*$ CO orbital in the chemisorption process, from measurements of its energy, which lies between 1.7 and 5.0 eV above

the Fermi level, depending on the metal.[20,22–27] However, these values reflect a complicated balance of different factors such as the metal–CO bonding character of the orbital receiving the electron (initial-state), final-state relaxation, and also CO⋯CO intermolecular interactions.[22] It is then difficult to simply relate the observed $2\pi^*$ features to the CO–metal surface bond strength.

A great variety of theoretical studies corroborate this overall description of the metal–CO bonding, although further analyses bring additional details. In particular, various results have shown

(1) Biloen, P.; Sachtler, W. M. H. *Adv. Catal.* **1981**, *30*, 165.
(2) Klier, K. *Adv. Catal.* **1982**, *31*, 243.
(3) Arakawa, H.; Takeuchi, K.; Matzuzaki, T.; Sugi, Y. *Chem. Lett.* **1984**, *1607*, 7610.
(4) Kip, B. S.; Hermans, E. G. F.; Prins, R. *9th International Congress of Catalysis*; Phillips, M. J., Ternan, M., Ed.; the Chemical Institute of Canada: Ottawa, 1988; Vol. 2, p 821.
(5) Post, D.; Baerends, E. J. *J. Chem. Phys.* **1983**, *78*, 5663.
(6) Lao, P. L.; Ellis, D. E.; Freeman, A. F.; Zheng, Q. Q.; Bader, S. D. *Phys. Rev. B* **1984**, *30*, 4146.
(7) Anderson, A. B.; Awad, M. K. *J. Am. Chem. Soc.* **1985**, *107*, 7854.
(8) Andzelm, J.; Salahub, D. R. *Physics and Chemistry of Small Clusters*; Jena, P., Rao, B. K., Khanna, S. N., Eds.; Nato Advanced Study Institute, Physics; Plenum: New York, 1987; Vol. 158, p 867.
(9) Koutecky, J.; Pacchioni, G.; Fantucci, P. *Chem. Phys.* **1985**, *99*, 87.
(10) Pacchioni, G.; Koutecky, J. *J. Phys. Chem.* **1987**, *91*, 2658.
(11) de Koster, A.; Van Santen, R. A. *Surf. Sci.* **1990**, *233*, 366.
(12) Drakova, D.; Doyen, G. *Surf. Sci.* **1990**, *226*, 263.
(13) Wong, Y. T.; Hoffmann, R. *J. Phys. Chem.* **1991**, *95*, 859.
(14) Blyholder, G. *J. Chem. Phys.* **1964**, *68*, 2772.
(15) (a) Lloyd, D. R.; Quinn, C. M.; Richardson, N. V. *Surf. Sci.* **1977**, *63*, 174. (b) Lloyd, D. R.; Quinn, C. M.; Richardson, N. V. *Surf. Sci.* **1977**, *63*, 574.
(16) Apai, G.; Wehner, P. S.; Williams, R. S.; Stöhr, J.; Shirley, D. A. *Phys. Rev. Lett.* **1976**, *37*, 1497.
(17) Shirley, D. A.; Stöhr, J.; Wehner, P. S.; Williams, R. S.; Apai, G. *Phys. Scr.* **1977**, *16*, 407.
(18) Allyn, C. L.; Gustafson, T.; Plummer, E. W. *Chem. Phys. Lett.* **1977**, *47*, 127.
(19) Allyn, C. L.; Gustafson, T.; Plummer, E. W. *Solid State Commun.* **1978**, *28*, 85.
(20) Rogosik, J.; Dose, V. *Surf. Sci.* **1986**, *176*, L847.
(21) Bagus, P. S.; Nelin, C. L.; Bauschlicher, C. W. *Phys. Rev. B* **1983**, *28*, 5423.
(22) Frank, K. H.; Sagner, H. J.; Koch, E. E.; Eberhardt, W. *Phys. Rev. B* **1988**, *38*, 8501.
(23) Johnson, P. D.; Wesner, D. A.; Davenport, J. W.; Smith, N. V. *Phys. Rev. B* **1984**, *30*, 4860.
(24) Rogosik, J.; Küppers, J.; Dose, V. *Surf. Sci.* **1984**, *148*, L658.
(25) Dose, J.; Rogosik, J. *Surf. Sci.* **1987**, *179*, 90.
(26) Johnson, P. D.; Hulbert, S. L. *Phys. Rev. B* **1987**, *35*, 9427.
(27) Rogosik, J.; Dose, V.; Prince, K. C.; Bradshaw, A. M.; Bagus, P. S.; Hermann, K.; Avouris, P. *Phys. Rev. B* **1985**, *32*, 4296.

† Ecole de Chimie.
‡ Université de Montréal.
§ Permanent address: Research Institute of Isotopes, Hungarian Academy of Sciences, H-1525 Budapest, POB 77 Hungary.

Density Functional Study of CO Chemisorption

J. Am. Chem. Soc., Vol. 114, No. 19, 1992 7453

that the 4σ orbital also participates in the bonding.[8,13,27-29] This participation has been described as a consequence of the polarization of the 5σ lone pair toward the O atom, in conjunction with the reverse polarization of 4σ.[28] The 5σ CO donation to the metal has been reported for top sites, but also for multibonded sites, where the amount of backdonation is, however, larger.[5,7,8,13,28]

On the basis of Hartree–Fock calculations of model clusters of Na, Mg, and Al, Bagus et al. have proposed a new interpretation of the metal–CO bonding, believing it to be essentially governed by a repulsive interaction between 5σ CO and the metal σ orbitals accompanied by a π attractive backdonation. These metals having no outer d electrons, the rehybridization, which occurs in order to reduce the σ repulsion, involves the 3s and $3p\sigma$ metal orbitals only. A similar concept has been used in Hartree–Fock studies of CO bonding with transition metal systems such as Cu, Fe, or Ni, where the metal–CO repulsive interaction also arises from the diffuse $sp\sigma$ metal orbitals.[31-34] The metal–CO bond is described by a major $d\pi$ metal to $2\pi^*$ CO donation, with a very small σ contribution to the covalent bond, especially when the metal atom involved has a filled $3d\sigma$ shell. This is the case for Cu systems. On the contrary, the CO 5σ donation is found to be significant when the metal $d\sigma$ subshell is empty or partially occupied (FeCO, Fe(CO)$_5$).[32,33] The ground states, nickel mono- and tetracarbonyls are proposed to arise through a mixing of $3d^9 4s$ and $3d^{10}$ Ni states, which weakens the σ repulsion.[32,33] Another description suggests the hybridization of the 4s and $3d\sigma$ Ni orbitals.[35,36]

Ab initio studies of PdCO, RhCO, and small Pd$_n$CO clusters, including or not including relativistic corrections and correlation effects, have led to a similar picture of a preponderant π bonding, coherent with d^{10} or d^9 metal atomic configurations for Pd and Rh systems, respectively.[9,10,37,38] When the average Pd configuration corresponds to some population of the 5(sp) orbitals, as found in a relativistic Hartree–Fock study of Pd$_8$CO (bridge site), some 5σ CO donation occurs through a partial rehybridization of the $d\sigma$ $sp\sigma$ orbitals.[39] In the same study, however, the evaluated σ donation is negligible for Pd$_2$CO, since each Pd atom retains a $4d^{10}$ configuration. Interestingly, the inclusion of relativistic corrections, which induces the contraction of the 5s and the expansion of the 4d Pd orbitals, has the effect of reinforcing the σ bonding.[39] In the same way, correlation effects increase σ donation as well as π backdonation, as shown by a comparison of the SCF and CI wavefunctions for Fe(CO)$_5$.[40]

To summarize the conclusions which can be drawn from the various Hartree–Fock based ab initio studies, we can say that the metal–CO bonding varies with (i) the metal, since an increased occupancy of the outer s orbital increases the repulsion; (ii) the ability of the metal $d\sigma$ $sp\sigma$ orbitals to hybridize, which governs the amount of σ donation; (iii) the amount of π backdonation.

The weakness of the σ donation, often reported in these studies, can be ascribed to a tendency to obtain more stable d^n configurations at the metal–CO equilibrium bond distance, which reduces the repulsion, and also to a low ability of the $d\sigma$ orbitals to hybridize with s and $p\sigma$ orbitals.

If we turn now to the results given by density functional (DF) studies, we get the same general characteristics for the metal–CO interaction, except that the σ bond is found to be effective, through a substantial amount of σ CO donation. Indeed, CO adsorption on Al and Cu clusters, studied with a Hartree–Fock–Slater LCAO method, is shown to first depend on an initial closed-shell repulsion, followed by 5σ CO donation and metal–$2\pi^*$ CO backdonation of equivalent magnitude.[5,41] For Cu clusters, both 4s and 4p orbitals are involved in the σ bonding. There are rearrangements in the 3d orbital population and the strong s/d mixing, allowed by symmetry, favors the participation of the 3d orbitals to both σ and π bonding. Comparison of the metal–CO interaction in RhCO and PdCO, based on an LCGTO-MCP-DF study, has shown that the initial repulsion is reduced by hybridization of the $4d\sigma$ 5s orbitals, which induces electron promotion from $4d\sigma$ to 5s orbitals and thus allows a charge transfer from the 5σ CO orbital (0.34 e for PdCO and 0.56 e for RhCO).[42] Local spin density (LSD) calculations on Pd$_8$CO, bridge site, have emphasized that the original σ repulsion is avoided through (i) the mixing of 4σ and 5σ characters, (ii) the destablization of antibonding Pd–5σ MOs, whose electrons are thus transferred to $d\pi$–$2\pi^*$ MOs, enhancing backdonation.[27] This transfer depends on the presence of empty orbitals at the top of the d "band", a possibility which is enhanced as the size of the cluster increases.

On the basis of all these results, it appears that the chemisorptive bond should depend on the configuration and the energetics of the metal atom(s) involved, but also on the metal–metal bonds in the cluster. Moreover, the initial repulsion, as well as the amount of σ and π contributions, will also depend on the sites considered and the geometry of the metal–adsorbate system. The comparison of CO chemisorption on Rh and Pd catalysts thus requires a valid description of the metal–metal and metal–CO bonds as a function of the geometry of the sites.

In this paper, we first report DF results for Rh$_2$ and Pd$_2$ dimers and for the bare model clusters Rh$_4$ and Pd$_4$. We then analyze the electronic structure, the geometry, and the vibrational and energetic properties of Rh$_4$CO and Pd$_4$CO clusters, used to model CO chemisorption at three different sites: top, bridge, and 3-fold.

II. Computational Details

The calculations have been performed within the linear combination of Gaussian type orbitals–model core potential–density functional formalism (LCGTO-MCP-DF),[43-45] using the deMon program package.[46,47] The grids used to fit the exchange-correlation potential and those used to evaluate the exchange-correlation contribution to the energy gradient are those reported previously.[42] The equilibrium geometries have been obtained by applying the analytical expression for the LCGTO-MCP-DF energy gradients.[48] Geometry optimizations have been performed within the local spin density (LSD) approximation, using the Vosko–Wilk–Nusair (VWN) parameterization for the exchange-correlation potential.[49] For energy calculations, nonlocal corrections to the LSD exchange[50] and correlation[51] have been added to the VWN potential.

Model core potentials (Rh^{15+}, Pd^{16+}) have been used for Rh and Pd atoms. The scalar relativistic effects are incorporated into the model potentials.[45] The 4p, 5s, 5p, and 4d orbitals have been treated explicitly. The contraction pattern of the valence electron orbital basis sets is (2211/2111/121) for Rh and Pd. For carbon and oxygen atoms, a triple-ζ plus polarization all electron basis set, with a (5211/411/1) contraction pattern, has been used. The auxiliary basis sets for the charge density (CD) and exchange-correlation (XC) fits are (3,4;3,4) for Pd and Rh, (5,2;5,2) for C and O. In the notation $(k_1, k_2; l_1, l_2)$ is the number of

(28) Andzelm, J.; Salahub, D. R. *Int. J. Quantum Chem.* **1986**, *29*, 1091.
(29) Tsai, M. H.; Rhodin, T.; Chambliss, D. D. *Phys. Rev. B* **1986**, *34*, 2688.
(30) Shinn, N. D. *Phys. Rev. B* **1988**, *38*, 12248.
(31) Bagus, P. S.; Hermann, K.; Bauschlicher, C. W. *J. Chem. Phys.* **1984**, *81*, 1966.
(32) Bauschlicher, C. W.; Bagus, P. S. *J. Chem. Phys.* **1984**, *81*, 5889.
(33) Bauschlicher, C. W.; Bagus, P. S.; Nelin, C. J.; Roos, B. O. *J. Chem. Phys.* **1986**, *85*, 354.
(34) Hermann, K.; Bagus, P. S.; Nelin, C. J. *Phys. Rev.* **1987**, *35*, 9467.
(35) Blomberg, M. R. A.; Brandemark, U. B.; Siegbahn, P. E. M.; Mathisen, K. B.; Karlström, G. *J. Phys. Chem.* **1985**, *89*, 2171.
(36) Siegbahn, P. E. M.; Blomberg, M. R. A.; Panas, I.; Wahlgren, U. *Theor. Chim. Acta* **1989**, *75*, 143.
(37) Smith, G. W.; Carter, E. A. *J. Phys. Chem.* **1991**, *95*, 2327.
(38) Blomberg, M. R. A.; Lebrilla, C. B.; Siegbahn, P. E. M. *Chem. Phys. Lett.* **1988**, *150*, 522.
(39) Pacchioni, G.; Bagus, P. S. *J. Chem. Phys.* **1990**, *93*, 1209.
(40) Lüthi, H. P.; Siegbahn, P. E. M.; Almlöf, J. *J. Phys. Chem.* **1985**, *89*, 2156.

(41) Post, D.; Baerends, E. J. *Surf. Sci.* **1982**, *116*, 177.
(42) Papai, I.; Goursot, A.; St-Amant, A.; Salahub, D. R. *Theor. Chim. Acta*, in press.
(43) Sambe, H.; Felton, R. H. *J. Chem. Phys.* **1975**, *62*, 1122.
(44) Dunlap, B. I.; Conolly, J. W. D.; Sabin, J. R. *J. Chem. Phys.* **1979**, *71*, 3396.
(45) Andzelm, J.; Radzio, E.; Salahub, D. R. *J. Chem. Phys.* **1985**, *83*, 4573.
(46) St-Amant, A.; Salahub, D. R. *Chem. Phys. Lett.* **1990**, *169*, 387.
(47) St-Amant, A. Ph.D. Thesis, Université de Montréal, 1991.
(48) Fournier, A.; Andzelm, J.; Salahub, D. R. *J. Chem. Phys.* **1989**, *90*, 6371.
(49) Vosko, S. H.; Wilk, L.; Nusair, M. *Can. J. Phys.* **1980**, *58*, 1200.
(50) Perdew, J. P.; Yue, W. *Phys. Rev. B* **1986**, *33*, 8800.
(51) Perdew, J. P. *Phys. Rev. B* **1986**, *33*, 8822.

Table I. Calculated Ground-State Properties of Rh$_2$ and Pd$_2$

molecular configuration (state)	r_e (Å)	ω_e (cm^{-1})	D_e (eV)^a calcd	D_e (eV)^a expt
Pd$_2$ $1\sigma_u 2\sigma_g$ ($^3\Sigma_u^+$)	2.46	209	1.35	0.74/1.13^b
Rh$_2$ $1\pi_u^3 1\delta_u^2 1\sigma_u$ ($^5\Pi_g$)	2.23	260	3.13	2.97^c

^{a} With respect to GS atoms ^{1}S Pd and ^{4}F Rh (nonspherical). ^{b} Reference 64. ^{c} Reference 65.

s-type Gaussians in the CD (XC) basis and k_2 (l_2) is the number of s-, p-, d-type Gaussians constrained to have the same exponent in the two bases.

The normal frequencies and normal coordinates have been determined by diagonalizing the Hessian matrix constructed by numerical differentiation of analytical gradients calculated at the equilibrium geometry. Infrared intensities have been calculated using the double harmonic approximation.[52] Both vibrational frequencies and infrared intensities have been calculated at the LSD level.
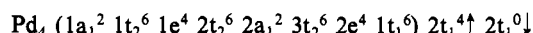
III. Results and Discussion

1. Rh$_2$ and Pd$_2$ Dimers. Dimers represent the smallest system which allows us to investigate the metal–metal bond. Theoretical effort devoted to the study of transition metal dimers has shown that the level of correlation required to describe these systems is typically very high. DF methods have provided the most accurate values for their equilibrium bond distances and vibrational frequencies.[53] The dissociation energies, obtained within the LSD scheme, are overestimated, but nonlocal corrections are now used, which greatly improve the energetics.[54-57] Among the 4d dimers, which have been far less studied than those of the 3d series, Pd$_2$ and Rh$_2$ have received very little attention. Early ab initio results yielded unrealistic equilibrium bond lengths (more than 0.15 Å larger than the bulk values), associated with very low dissociation energies.[58-60] More recently, low-lying electronic states of Rh$_2$ and Pd$_2$, together with their spectroscopic properties, have been investigated at a high level of the ab initio methodology, i.e., MCSCF calculations, followed by MRSDCI and relativistic CI.[61,62]

It is thus very interesting to compare these results with those we have obtained with the LCGTO-MCP-DF method. The ground-state (GS) properties of Pd$_2$ and Rh$_2$ are reported in Table I, together with the available experimental values for their dissociation energies (D_e). The GS electronic configuration for the valence electrons is $1\sigma_g^2 1\delta_g^4 1\pi_g^4 1\pi_u^4 1\delta_u^4 1\sigma_u 2\sigma_g$ for Pd$_2$ and $1\sigma_g^2 1\delta_g^4 1\pi_g^4 1\pi_u^4 1\delta_u^2 1\sigma_u 2\sigma_g^2$ for Rh$_2$. Only the open-shell part is reported in Table I. The Pd$_2$ GS is similar to that obtained from the MRSDCI calculations.[61] For Rh$_2$, the GS is different, with π_u, δ_u, and σ_u holes for the present work, instead of π_g, δ_u, and σ_u holes.[62] Although ab initio CI and DF calculations constitute two different approaches to the problem of electron correlation, their descriptions of the GS properties of these two dimers are very comparable. Indeed, our values compare very well with Balasubramanian's for the equilibrium bond distances (2.48 and 2.28 Å) and stretching frequencies (160 and 267 cm^{-1}) for Pd$_2$ and Rh$_2$, respectively. Both studies show the same tendency of a larger shortening for the Rh–Rh bond with respect to the bulk value (2.69 Å) than for the Pd–Pd bond (2.75 Å). Moreover, they reflect the larger metal–metal bond strength for Rh$_2$ than for Pd$_2$,

corroborated by the larger value of the Rh–Rh stretching frequency. The Mulliken population analysis for the GS of the dimers gives the following gross atomic populations: Pd 5s$^{0.58}$ 5p$^{0.04}$ 4d$^{9.38}$ and Rh 5s$^{1.13}$ 5p$^{0.01}$ 4d$^{7.86}$. There is thus a large 5s contribution to the metal–metal bond, for both dimers. The 4d^{10} Pd atoms undergo rehybridization of their dσ orbitals in order to form the metal–metal 5s bonding combination 2σ_g. The 4d^8 5s^1 GS configuration for Rh facilitates the formation of this σ bonding MO, which is doubly occupied. Thus, for both dimers, the initial repulsion is overcompensated by σ and π bonding. This description is in agreement with that derived from Balasubramanian's work, which gives very similar gross atomic populations for the ground states and leads to the conclusion that d^{n-1} s^1 was the predominant configuration for both dimers. The dissociation energies obtained from DF calculations, including nonlocal corrections, remain at the upper limit of the experimental evaluations but the agreement is far more than qualitative. In particular, these results show that we do find effective metal–metal bonds, which was not the case for most previous ab initio calculations, yielding nonbonded or little-bonded dimers, with predominant d^n configurations.[38,58,59,63] Moreover, the relative bond strength of Rh$_2$ versus Pd$_2$ is very well reproduced, which is a favorable factor for a comparative study of chemisorption on Rh and Pd clusters. This trend was also reproduced by Balasubramanian's results, which led to calculated D_e, with respect to the GS atoms of 2.10 eV for Rh$_2$ and 0.85 eV for Pd$_2$ (evaluated on the basis of the published results). In agreement with this author, we find that the bond order is 3 for Rh$_2$ and 1 for Pd$_2$, in their ground states. Other configurations have been explored for these dimers. The lowest excited state for Pd$_2$ is $^1\Sigma_g^+$ ($1\sigma_u^2$), 0.41 eV higher than the GS, with a Pd–Pd bond length of 2.64 Å and a D_e of 0.95 eV with respect to two ^{1}S atoms. For Rh$_2$, there are several low-lying configurations. Among them, the lowest one corresponds to a $^3\Sigma_g^-$ ($1\delta_u^2$) at 0.79 eV from the GS, with a 2.22-Å bond length.

2. Rh$_4$ and Pd$_4$ Clusters. These clusters have been studied in a tetrahedral geometry, as a model for a (111) structure. The metal–metal bond distances have been fixed to the bulk values, i.e., 2.69 Å for Rh$_4$ and 2.75 Å for Pd$_4$. The GS of these model clusters, calculated with spin polarization, are described by the following configurations (only 4d and 5s electrons are indicated):

$$\text{Pd}_4 \ (1a_1^2 \ 1t_2^6 \ 1e^4 \ 2t_2^6 \ 2a_1^2 \ 3t_2^6 \ 2e^4 \ 1t_1^6) \ 2t_1^4{\uparrow} \ 2t_1^0{\downarrow}$$

$$\text{Rh}_4 \ (1a_1^2 \ 1t_2^6 \ 1e^4 \ 2t_2^6 \ 2a_1^2 \ 2e^4 \ 3t_2^6) \ 1t_1^3{\uparrow}2t_1^3{\uparrow} \ 1t_1^0{\downarrow} \ 2t_1^0{\downarrow}$$

The total Mulliken population analysis leads to the following atomic configurations: Pd 5s$^{0.54}$ 5p$^{0.12}$ 4d$^{9.34}$ and Rh 5s$^{0.59}$ 5p$^{0.17}$ 4d$^{8.24}$. It is known that the bulk metals have no magnetic properties. In fact, if the geometry of the cluster is allowed to relax, singlet states are found as ground states for both models. However, all calculations including or not including spin polarization lead to quite similar gross atomic populations as those indicated. Comparison with the Rh$_2$ and Pd$_2$ gross atomic populations indicates that increasing the number of atoms makes the Rh and Pd atomic configurations closer, with non negligible 5p contributions and intermediate d^n/d^{n-1} (sp)^1 configurations. The calculated binding energy per atom is 2.32 eV for Rh$_4$ and 1.58 eV for Pd$_4$. The ratio of these values (1.47) compares very well with the ratio of the experimental cohesive energies of the bulk material (1.54, i.e., Rh 6.0 and Pd 3.9 eV). This indicates that, even though we cannot discuss absolute energies on the basis of such small cluster calculations, their comparison for different metals should be valid.

3. Pd$_4$CO and Rh$_4$CO Models. (a) Structural and Vibrational Properties. The Rh$_4$ and Pd$_4$ parts have been kept fixed, with bulk bond distances, while CO geometry and orientation were optimized for the three possible sites: 3-fold, bridge, and top. After optimization, the 3-fold and bridge models keep their initial symmetries, respectively C_{3v} and C_{2v}. In contrast, CO in an on-top position does not remain on the C_3 axis. It tilts away from the

(52) Herzberg, G. *Infrared and Raman Spectra of Polyatomic Molecules*; Van Nostrand: New York, 1945.
(53) Salahub, D. R. *Adv. Chem. Phys.* **1987**, *69*, 447.
(54) Becke, A. D. In *The challenge of d and f electrons*; Salahub, D. R., Zerner, M. C., Eds.; ACS: Washington, 1989; p 165.
(55) Mlynarski, P.; Salahub, D. R. *Phys. Rev. B* **1991**, *43*, 1399.
(56) Ziegler, T. *Chem. Rev.* **1991**, *91*, 651.
(57) Godbout, N.; Salahub, D. R.; Andzelm, J.; Wimmer, E. *Can. J. Chem.*, in press.
(58) Shim, I. *Mat.-Fys. Medd.-k. Dan. Vidensk. Selsk.* (Sixteen Research Reports of Niels Bohr Fellows) **1985**, *41*, 147.
(59) Shim, I.; Gingerich, K. A. *J. Chem. Phys.* **1984**, *80*, 5107.
(60) Basch, H.; Cohen, D.; Topiol, S. *Isr. J. Chem.* **1980**, *19*, 233.
(61) Balasubramanian, K. *J. Chem. Phys.* **1988**, *89*, 6310.
(62) Balasubramanian, K.; Liao, D. W. *J. Phys. Chem.* **1989**, *93*, 3989.

(63) Mains, G. J.; White, J. M. *J. Phys. Chem.* **1991**, *95*, 112.
(64) Lin, S. S.; Strauss, B.; Kant, A. *J. Chem. Phys.* **1969**, *51*, 2282.

Table II. Optimized M–C and C–O Bond Distances,[a] Vibrational Frequencies,[b] and Net CO Charge for M_4CO Clusters

M	site	M–C (expt)[c]	C–O (expt)[c]	ν(C–O) (intensity) (expt)[c]	ν(M–C) (expt)[c]	q(CO)
Pd	top	1.848	1.155	2090 (940) (2020–2080)[d]	455	−0.10
	bridge	1.883 (1.93 ± 0.07)[d]	1.185 (1.15 ± 0.1)	1879 (877) (1880–1895)	431	−0.20
	3-fold	1.960 (2.05 ± 0.04)[f]	1.206 (1.15 ± 0.05)	1738 (420) (1805–1820)	403	−0.40
Rh	top	1.826 (1.95 ± 0.10)[f]	1.164 (1.07 ± 0.10)	2038 (980) (1990–2010)	489 (460)	−0.10
	bridge	1.875 (1.95 ± 0.10)[g]	1.200 (1.15 ± 0.10)	1790 (670) (1820–1840)	437 (400)	−0.20
	3-fold	1.976	1.214	1693 (480) (1680–1690)[e]	407	−0.40

[a] In Å. [b] In cm^{-1}. [c] Values taken from ref 66. [d] Measured at Θ = 0.5. [e] In the presence of coadsorbed water. [f] Measured at Θ ≤ 0.3. [g] Measured at Θ ≤ 0.75.

Table III. Energies (E), M, C, and O Atomic Contributions, and Mulliken Overlap Populations (OP) for the 4σ̄, 5σ̄, and 1π̄ MOs of Pd_4CO and Rh_4CO, Derived from the 4σ, 5σ, and 1π MOs of Free CO

MOs		Pd_4CO top	bridge	3-fold	Rh_4CO top	bridge	3-fold	free CO
4σ̄	E (eV)	−14.38	−14.95	−14.86	−13.77	−14.02	−14.34	−14.20
	C (%)	43	57	62	44	56	61	20
	O (%)	50	26	19	48	26	19	80
	M (%)	7	17[a]	19[a]	8	18[a]	20[a]	
	M–C OP	−0.01	0.13	0.08	0.07	0.33	0.19	
	C–O OP	−0.08	−0.09	−0.08	−0.07	−0.07	−0.05	0.00
5σ̄	E (eV)	−12.03	−12.00	−11.39	−11.36	−11.00	−10.87	−9.08
	C (%)	37	23	19	34	23	19	91
	O (%)	36	59	64	38	58	63	9
	M (%)	27	19[a]	17[a]	28	19[a]	18[a]	
	M–C OP	0.39	0.11	0.00	0.50	0.15	0.02	
	C–O OP	0.00	−0.06	−0.12	0.01	−0.06	−0.11	−0.23
1π̄	E (eV)	{−11.56, −11.55}	{−11.24, −11.78}	{−11.06, −11.06}	{−10.84, −10.84}	{−10.30, −10.70}	{−10.42, −10.42}	−11.86
	C (%)	33	42	45	34	42	44	28
	O (%)	64	42	38	62	43	39	72
	M (%)	3	16[a]	17[a]	4	15[a]	17[a]	
	M–C OP	0.07	0.14	0.10	0.09	0.15	0.12	
	C–O OP	0.86	0.73	0.70	0.83	0.74	0.70	0.87

[a] Sum of contributions for two metal atoms (bridge) or three metal atoms (3-fold).

axis and becomes roughly perpendicular to a triangular facet, yielding a global C_s symmetry. The calculated M–C (M denotes metal) and C–O bond lengths, together with the related stretching frequencies, are reported in Table II. They are compared with available experimental data on supported particles or single-crystal (111) surfaces. The experimental geometries are determined on surfaces, most often at intermediate or high coverage (Θ) values. They are thus not directly comparable with our calculations. However, their comparison may be useful if it is kept in mind that large coverage values increase the intermolecular CO interactions and thus increase the metal–CO bond distances. The experimental ν(C–O) values reported in Table II correspond to singletons, except when indicated. Singletons are difficult to obtain and their ν(C–O) values may depend on experimental conditions.[65] This explains why only frequency ranges are indicated. Examination of the results leads to two principal remarks: (1) for both metals, the calculated M–C and C–O bond lengths increase in going from top to bridge to 3-fold sites. In the same way, the related calculated stretching frequencies decrease. (2) Rh–C bonds are shorter than Pd–C bonds, for all sites, whereas the corresponding C–O bonds follow the reverse order. The M–C and C–O stretching frequencies reflect this behavior.

It is expected, for geometric reasons, that the metal–adsorbate bond distance increases with the number of bonded metal atoms, and indeed, this is corroborated by LEED results.[67-70] The low precision generally obtained for the measurement of C–O bond lengths does not allow any conclusion for Pd substrates. However, it is clear, from measurements on the Rh substrates, that the C–O bond length increases as Rh–C is lengthened. Although they are obtained at different coverage values, the Rh–C bond length measured for the bridge site is unambiguously larger than the Pd–C bond length. There are no experimental data available, either for the top site on Pd, which is only populated near saturation, or for the 3-fold site on Rh, which has not yet been observed. The calculated lengthening of the C–O bond, concomittant with that of the M–C bond, is reflected by the net decrease of the calculated ν(C–O) values from top to 3-fold site and from Pd to Rh substrate. The same trends can be derived from the analysis of the experimental frequencies. Moreover, the gaps between the calculated ν(C–O) at the three sites and their differences for Pd and Rh clusters at the same site are fully consistent with the experimental data.

The lengthening of C–O, when moving from top to 2- and 3-fold sites, may be related to the increased metal–2π* backdonation, which weakens progressively the C–O bond. If we use the Mulliken population analysis as a qualitative index for the mixing of metal and CO orbitals, we see that the total CO electronic population indeed increases with the number of bonded metal atoms (Table II). The evolution is similar for Pd and Rh clusters.

(65) Cocke, D. L.; Gingerich, K. A. *J. Chem. Phys.* **1974**, *60*, 1958.
(66) Goursot, A. *Metal–Ligand Interactions: From Atoms to Clusters to Surfaces*: Salahub, D. R., Russo, N., Eds.; Kluwer: Boston, in press.
(67) Behm, R. J.; Christmann, K.; Ertl, G. *J. Chem. Phys.* **1980**, *73*, 2984.

(68) Ohtani, H.; Van Hove, M. A.; Somorjai, G. A. *Surf. Sci.* **1987**, *187*, 372.
(69) Koestner, R. J.; Van Hove, M. A.; Somorjai, G. *Surf. Sci.* **1981**, *107*, 439.
(70) Van Hove, M. A.; Koestner, R. J.; Frost, J. C.; Somorjai, G. A. *Surf. Sci.* **1983**, *129*, 482.

Comparison between the two metals has to be made at a more detailed level. It is not easy to delineate σ and π effects since the four metal atoms are involved in the bonding with CO. The analysis of the gross atomic populations for the 3-fold site models shows that the sp_σ orbitals of CO lose a significant amount of charge (0.7 e for Pd$_4$CO, 0.8 e for Rh$_4$CO), whereas the $p\pi$ CO orbitals gain 1.1 and 1.2 e for the Pd and Rh clusters, respectively. This π backbonding involves s, p, and d metal orbitals. The amounts of charge transferred are slightly larger for the Rh cluster. The same conclusion can be drawn for the two other models.

(b) Metal–CO Bonding Interactions. Let us now turn to a more detailed description of the wave functions, aiming at the analysis of the differences between Pd and Rh models, for the three sites. The cluster MOs, derived from 4σ, 5σ, and 1π CO MOs, are described in Table III. Their energies and composition at the three sites are given for Pd$_4$CO, Rh$_4$CO, and free CO, together with the M–C and C–O overlap populations, which are used as indices of the bond strength. The comparison of the C and O contributions to $4\tilde\sigma$ and $5\tilde\sigma$ with respect to the free CO molecule shows a strong mixing of 4σ and 5σ characters. As already mentioned for Pd$_8$CO (bridge site),[27] the $5\tilde\sigma$ orbital polarizes strongly toward the O atom. This effect increases with the number of metal–carbon bonds, the smaller polarization being for the top site. In response, $4\tilde\sigma$ polarizes toward the carbon, increasingly from the top to the 3-fold site. It is worthy to note that the metal contribution to $5\tilde\sigma$ is significantly larger for the top site model than for the others, for which this MO is more distributed toward the oxygen. In contrast, $4\tilde\sigma$ polarizes more significantly toward the metal and carbon atoms for the bridge and 3-fold sites. Examination of the M–C overlap population shows that it increases, for $4\tilde\sigma$, from top to multibonded sites, with a maximum for the bridged model. For $5\tilde\sigma$, the substantial overlap population obtained for the top species reflects an important metal–CO σ bonding interaction, which decreases very rapidly when the CO coordination increases. The C–O overlap populations indicate a tendency of $4\tilde\sigma$ to acquire some antibonding C–O character, whereas $5\tilde\sigma$ reduces it, with respect to the free CO molecule, especially for the top site model. Finally, we see that the sum of the metal contributions to $4\tilde\sigma$ and $5\tilde\sigma$ remains quasi constant for all models. This shows that, in all cases, there is a σ donation from CO to the metal clusters, accompanied by a strong polarization of the σ CO orbitals. However, charge donation from CO to the metal substrates does not necessarily mean contribution to the metal–CO bonding. This is particularly true for the 3-fold site models, for which the metal–C overlap population of $5\tilde\sigma$ is very small, most of the charge transferred to the cluster being distributed among the in-plane 4d orbitals of the three metal atoms. The evolution of $4\tilde\sigma$ and $5\tilde\sigma$ MOs is similar for Pd$_4$CO and Rh$_4$CO clusters. The metal contributions to these MOs are comparable, but the metal–C bonding interactions are systematically larger for the Rh clusters. The contribution of the metal orbitals to the $1\tilde\pi$ MO is negligible for the top site models. For the other sites, $1\tilde\pi$ polarizes strongly toward the C atom and the metal neighbors, whose contribution becomes substantial. Due to the delocalization of the metal orbitals involved, the metal–C overlap population remains small. $1\tilde\pi$ is slightly destabilized with respect to free CO, due to the weakening of the C–O bond, consecutive to its lengthening, which increases from top to 3-fold site. Therefore, the main contribution to the π bonding between CO and the metal clusters is achieved through bonding combinations of the $2\pi^*$ CO MOs with metal orbitals. The $2\pi^*$ orbital contributes to a large number of occupied metal MOs. Its contribution increases strongly with the number of metal–CO bonds and is close for Rh and Pd clusters. About 0.9 (1.0), 1.5 (1.5), 1.7 (1.8) electrons are transferrred to the $2\pi^*$ orbital of Pd$_4$CO (Rh$_4$CO), for the top, bridge, and 3-fold site models, respectively. Bond orders are helpful to describe bonding properties between two atoms and their evolution in different systems.[71] The M–C and C–O Mayer bond orders for the studied models are compared in Table IV. The M–C bond orders reflect the decrease of the

metal–CO bond strength with increasing C coordination and its larger value for Rh–CO with respect to Pd–CO. The C–O bond order values show that the adsorption of CO leads to the weakening of the C–O bond with respect to free CO, the importance of this effect being correlated with the site coordination. This result is fully consistent with an increase of the C–O bond length and the decrease of its stretching frequency from top, to bridge, to 3-fold site models.

For coordinated CO species, it is typical that the ionization potentials of $5\tilde\sigma$ and $1\tilde\pi$ are practically degenerate while that of $4\tilde\sigma$ is not significantly different from the value for a free CO molecule. Although DF eigenvalues are not directly related to IPs, we see that the calculated energies of $4\tilde\sigma$, $5\tilde\sigma$, and $1\tilde\pi$ reproduce the experimental trends. The interpretation of the $5\tilde\sigma$ stabilization cannot be merely reduced to the effect of its participation in metal–CO σ bonding. Indeed, although this stabilization is smaller for the 3-fold site model than for the others, it remains substantial, despite the nonbonding character of the σ interaction of CO with the three metal atoms. The strong mixing of 4σ and 5σ characters is probably the more decisive factor, for the 3-fold site model, conjugated with the decrease of the antibonding CO character. The participation of small bonding metal–metal contributions must not be neglected. For the top site models, the electron donation from $5\tilde\sigma$ CO remains the most important factor, while the weight of the others has to be lowered. The bridge site case corresponds to an in between situation. To conclude this description of the metal–CO bonding, let us mention that there are antibonding metal–5σ contributions, as counterparts of the bonding $5\tilde\sigma$ MOs. The importance of emptying these orbitals, to reduce Pauli repulsion, has been discussed elsewhere.[27] For the multibonded models, these levels are virtual, the lowest one being the LUMO. For the top site models, two occupied levels have metal–5σ CO antibonding characters. However, it is only for the Pd$_4$CO top site that the metal contribution to the antibonding interaction is nonnegligible (10%).

(c) Characteristics of CO Chemisorption: Site Selection. DF results, using local exchange and correlation functionals, have shown a net dependence of the CO chemisorption energies on the size of the clusters.[8,27] First attempts to evaluate gradient corrected binding energies for Ni clusters have shown, however, that the experimental values are reproduced already for 4-atom clusters.[72,73] For the present study, we expect that examination of the differences between sites for the same cluster or between Rh and Pd models will give good insight into the trends which determine the energetics of chemisorption on real systems. The calculated adsorption energies for Rh$_4$CO and Pd$_4$CO clusters are compared in Table IV. The atomic configurations for the metal atom(s) bonded to CO, evaluated from the Mulliken populations analysis, are also reported.

For Pd$_4$CO, the binding energies to the three sites are different. Adsorption at the 3-fold site is favored, while the top site is found to be the least probable. On the contrary, the binding energies for the Rh$_4$CO clusters are very close to each other, with a preference for top and bridge sites. IR and TPD spectra measured

Table IV. Calculated CO Dissociation Energies (D_e),[a] Metal Atomic Configurations, and M–C and C–O Bond Orders (BO) at the Different Sites

	Pd$_4$CO			Rh$_4$CO		
	top	bridge	3-fold	top	bridge	3-fold
D_e (calcd) (expt value)	30.4 (20–25)	41.2 (35–40)	54.2 (35–40)	53.3	54.4	49.5
metal configuration	$s^{0.95}$ $p^{0.26}$ $d^{8.81}$	$s^{0.78}$ $p^{0.17}$ $d^{9.14}$	$s^{0.51}$ $p^{0.10}$ $d^{9.30}$	$s^{0.91}$ $p^{0.22}$ $d^{8.11}$	$s^{0.75}$ $p^{0.23}$ $d^{8.26}$	$s^{0.57}$ $p^{0.11}$ $d^{8.31}$
M–C BO	1.03	0.95	0.69	1.37	1.21	0.79
C–O BO[b]	2.29	2.03	1.85	2.20	1.90	1.78

[a] In kcal mol^{-1}. [b] 2.54 for free CO.

(71) Mayer, I. *Chem. Phys. lett.* **1983**, *97*, 270.

(72) Fournier, R.; Salahub, D. R. *Surf. Sci.* **1991**, *245*, 263.
(73) Mlynarski, P.; Salahub, D. R. *J. Chem. Phys.* **1991**, *95*, 6050.

Density Functional Study of CO Chemisorption

J. Am. Chem. Soc., Vol. 114, No. 19, 1992 7457

for Pd(111) surfaces indicate that CO adsorbs exclusively at 3-fold sites for low coverage values. At intermediate coverage, both bridge and 3-fold sites are occupied and the average binding energy at these two sites is 35–40 kcal mol^{-1}.[74,75] The top site is only populated at high coverage,[76] and the related CO binding energy can be estimated at 20–25 kcal mol^{-1}.[74] The calculated values compare surprisingly well with the experimental results, since adsorption energies at low coverage should be somewhat larger than at half-coverage. There is no experimental value for CO adsorption energies on Rh surfaces or supported particles. However, IR and TPD experiments indicate that the top site is first occupied on Rh(111) surfaces, followed by the bridge site at increasing coverage. CO adsorption at the 3-fold site has not yet been reported without the presence of a coadsorbate. However, it is not to be ruled out completely, due to the low intensity of the multibonded C–O stretching bands and also to the broadness of the band assigned to the bridged CO vibration (ca. 100 cm^{-1}). For example, CO adsorption at the 3-fold site on Pt/Al$_2$O$_3$ particles has been demonstrated only very recently from thermal desorption experiments: the broad IR band associated with the bridged species decomposed into two separate bands assigned to bridge and 3-fold sites.[77]

However, beyond the absolute values of the binding energies and their comparison with experimental results obtained for particular infinite surfaces, we can say that the site preference is pronounced for Pd$_4$ and very weak for Rh$_4$. Moreover, since multiple Pd–CO bonds are favored, we can infer that the π bonding, involving essentially d electrons, is more efficient than the Pd–CO bond of the top site, which concerns more sp$_\sigma$ electrons. In contrast, we find that the energy differences between the sites on the Rh$_4$ model are small, as if the different types of bonding, involving either more sp$_\sigma$ or more p$_x$d$_\pi$ Rh orbitals, were of equivalent strength.

Examination of the configurations of the metal atom(s) to which CO is bonded brings additional insight. The metal configuration varies strongly with the adsorption site, but its variation with the nature of the metal is negligible, except for the one d-electron difference. This shows that the metal configuration is thus characteristic of the adsorption site, independent of the metal itself. It is tempting to correlate these two characteristics, the binding energies to the sites (different for Pd$_4$CO, similar for Rh$_4$CO) and the metal site configuration, which appears to be typically related to the nature of this site. The correlation is apparent if we admit that the metal atoms on the surface, each of them having a configuration close to (sp)$^{0.6}$ d$^{n-0.6}$ (found for M$_4$ bare clusters), have some "memory" of the relative energies of various ground and excited states of the isolated atom, when responding, locally, to the CO chemisorption. Indeed, we know what makes the difference between the bonding capability of Pd and Rh atoms.[42] Pd has a 4d^{10} GS configuration which favors π bonding with CO. In order to allow σ bonding involving the d orbitals, it is necessary to break the closed d$_\sigma$ shell by promoting a d$_\sigma$ electron into an s (or p$_\sigma$) orbital. The cost of this is governed by the large energy difference between the ground state and the 4d^9 5s^1 configuration, which amounts to about 1 eV. In contrast, Rh has a 4d^8 5s^1 GS configuration, which, as we have seen previously, favors σ bonding. However, its lowest excited configuration, i.e., 4d^9, is only 0.35 eV higher, which means that the energetic cost for changing to any configuration intermediate between 4d^8 5s^1 and 4d^9 will be relatively low. Under the assumption we have made that CO induces essentially a local rearrangement on the metal atom(s) of the site, we thus expect that Pd atoms will adopt more easily configurations with the lowest 5s and highest 4d populations. This is the case for the 3-fold adsorption site, where the metal atoms bonded to CO have the lowest 5s occupancy, very close to that of the atoms in the bare cluster. In fact, the fourth atom of the cluster also participates in the bonding and has an even lower 5(sp)

population (0.30 for Pd and 0.36 for Rh). On the contrary, the Pd top site will be disfavored since it requires the promotion of 1.2 electrons from the 4d$_\sigma$ into the 5(sp$_\sigma$) orbitals. We may thus understand why the 3-fold site of Pd$_4$CO has the highest binding energy whereas the top site is unlikely and the bridge site is in between. The situation for Rh models is different, due to the facility of the Rh atom to adopt either low or high 5(sp) population. This correlates with the close binding energies obtained for the three sites with a slightly less favorable energy for the 3-fold site which corresponds to a larger contribution of the 4d^9 configuration.

Even if strongly localized, the perturbation induced by CO chemisorption also involves the first neighbor atoms of those bonded to CO. Bonding of CO at bridge and 3-fold sites is more delocalized than at the top site and will thus concern more neighboring metal atoms. In fact, the assumption that chemisorption is, to a first approximation, a localized process is supported by the fact that, for the top site which corresponds to the more localized M–CO bonding, the atomic configurations of the other three metal atoms are not much changed with respect to those of the bare M$_4$ cluster. Indeed, their 5(sp) and 4d orbitals loose less than 0.1 electron for each group, which contributes to the increased sp population of the top site atom, together with charge transferred from its own 4d orbitals. For the bridge and 3-fold site models, the atoms not directly bonded to CO contribute more substantially to the electronic rearrangements induced by the bonding with CO.

A four-atom cluster is certainly too small to fully quantify this rough picture of concerted transfers of the electronic population into the orbitals of the metal site and into those of its neighbors demanded by the bonding process. Further calculations on larger size clusters will help to complement our understanding in that direction. However, increasing the size of the bare cluster will lower the sp population (to about 0.3–0.4 for bulk Pd from band calculations[78] and thus increase that of 4d (to $(n - 0.3)/0.4$) but will keep the Rh and Pd atomic configurations similar. We thus expect that what we could call the "site configurations" will remain nearly independent of the cluster size and rather similar for Rh and Pd sites.

On the basis of these results, we thus propose that the site preference for the adsorption of noninteracting CO molecules is governed by the energetic properties specific to the metal atom(s) of the site, its neighbors being attributed the role of a reservoir of electronic charge used, when necessary, to adopt the configuration required by the bonding with CO. It would be of clear interest to see whether this reasoning can be extended to neighboring or more distant atoms in the periodic table.

Finally, we would like to emphasize that the above explanation for the site preference does not depend on any particular description of the spatial orientation of sp$_\sigma$–d$_\sigma$ hybrid orbitals (although some mixing does occur in our calculations), but only on the effective electronic configuration for the atom in the cluster. The concept of hybridization has been discussed by many authors[31–36,38] as a way to reduce the σ repulsion between a metal atom and an incoming ligand. However, the spatial rearrangement of the charge density does not necessarily imply substantial changes in the individual populations of the original s and d orbitals.[35,36] The argument that hybridization is not a good way to decrease the repulsion if it costs too much energy to be realized has also been used in various analyses on Ni, Cu, or Pd compounds.[35,36,38] In the case of our Pd$_4$CO and Rh$_4$CO models, we have seen that the bonding of CO with one or several metal atoms can induce substantial changes in the effective electronic configurations of the metal atom(s) of the site. What is new in our result is that these adsorbate-induced changes are found to be specific to the site of adsorption and of the adsorbed molecule. This peculiarity can explain the site preference, different for Rh and Pd surfaces, owing to the assumption that the metal atom(s) of the site, although bonded to other metal atoms, has some "memory" of the energetic properties it had as an isolated atom, i.e., relative energies

(74) Ladas, S.; Poppa, H.; Boudart, M. *Surf. Sci.* **1981**, *102*, 151.
(75) Gillet, E.; Channakhone, S.; Matolin, V. *J. Catal.* **1986**, *97*, 437.
(76) Bradshaw, A. M. *Surf. Sci.* **1978**, *72*, 513.
(77) Haaland, D. M. *Surf. Sci.* **1987**, *185*, 1.

(78) Anderson, O. K. *Phys. Rev. B* **1970**, *2*, 883.

of the ground and excited configurations.

IV. Conclusions

Calculated chemisorption properties of CO on Rh and Pd model clusters have been compared for two purposes. The first one was to verify whether DF calculations on small model clusters could reproduce experimental trends for the geometries and vibrational frequencies of CO adsorbed on Rh and Pd catalysts, with variation of both adsorption sites and metal substrates. Our second aim was more ambitious since it concerned a possible correlation between the site selection for CO chemisorption on Rh and Pd surfaces and some fundamental properties of these metals.

In a first step, the description of the metal–metal bond by the LCGTO-MCP-DF method has been checked by calculations on Rh_2 and Pd_2 dimers. Our results show that this description, at least for the ground states, is in good agreement with that given by very accurate CI calculations. It is worthwhile to note that these results show a stronger metal–metal bond for Rh_2 than for Pd_2, in agreement with experiment. We have then confirmed that LSD calculations on M_4CO models were able to reproduce the observed trends of the metal–CO and C–O bond lengths and stretching frequencies for an adsorbed CO molecule at three different sites of Rh and Pd (111) surfaces. All these results are consistent with a larger Rh–CO than Pd–CO bond strength.

The analysis of the wave functions of the different models has confirmed that the 4σ and 5σ CO MOs are strongly mixed, especially for multibonded sites, and that a σ donation from CO to the clusters occurs for all models. However, the σ charge transferred to the metal substrate is mainly distributed among metal orbitals in the surface for the adsorption at 3-fold site, whereas it provides the σ bonding between CO and the metal atom of the top site model. As reported previously, the metal–CO π bonding is achieved through bonding combinations of occupied metal MOs and $2\pi^*$ CO contributions, which increase with the coordination number of the site and are larger for Rh than for Pd models.

The gradient corrected binding energies of CO are clearly different for the three sites of Pd clusters, favoring the adsorption at the most highly coordinated site. In contrast, these energies are rather similar for the three sites of the Rh clusters. Examination of the Mulliken gross atomic populations has led to unexpected conclusion that the atomic configuration of the metal atom(s) bonded to CO is a characteristic of the adsorption site and is independent of the metal itself (except for the one d-electron difference between Rh and Pd). These results can be rationalized if we assume that the metal atom(s) of the surface, on which CO chemisorbs, has some "memory" of the energies of the isolated atom(s), which determines its ability to adopt a particular configuration and hence its bonding capability.

In other words, CO chemisorption can be viewed as local electronic rearrangements in the orbitals of the metal atom(s) of the site, in which the neighboring atoms can participate. These rearrangements, imposed by the bonding with CO, are different with different sites, and CO will bond preferentially to the site whose specific configuration is the closest to the GS configuration of the isolated metal atom. Small or large differences between adsorption energies at different sites could thus be related to the relative energies of ground and excited configurations of the isolated atom. Further calculations are in progress to verify if this concept of site configuration applies independently of the cluster size and if our interpretation can be extended to other metal systems.

Homolytic Bond (H–A) Dissociation Free Energies in Solution. Applications of the Standard Potential of the (H+/H·) Couple

Vernon D. Parker

Contribution from the Department of Chemistry and Biochemistry, Utah State University, Logan, Utah 84322-0300. Received March 20, 1992

Abstract: Free energies of solvation [$\Delta G_{solv}(gas)_{aq}$'s] of the noble gases in water are linearly related to the atomic radii. These data allow $\Delta G_{solv}(H^·)_{aq}$ to be calculated from the correlation line. The standard potential [$E°(H^+/H^·)_{aq}$] for reduction of the proton in water (reaction i) was then determined using eq ii. The value of $E°_{NHE(aq)}(H^+/H^·)_{aq}$ was observed to be –2.42

$$H^+ + e^- \rightleftarrows H^· \tag{i}$$

$$E°_{NHE(aq)}(H^+/H^·)_{aq} = -(\Delta G_{solv}(H^·)_{aq} + \Delta G_f(H^·)_{gas})/F \tag{ii}$$

V. Similarly, it was shown that the standard electrode potentials for the (H+/H·) couple in other solvents (S) can be determined using eq iii. The standard potentials for the (H+/H·)S couple are directly applicable in thermochemical cycles to the determination

$$E°_{NHE(S)}(H^+/H^·)_S = -(\Delta G_{solv}(H^·)_S + \Delta G_f(H^·)_{gas})/F \tag{iii}$$

of the differences in free energies of heterolysis and homolysis of bonds in solution. The bond dissociation energies obtained in this manner are subject only to the experimental errors in the determination of anion redox potentials $E(A^·/A^-)_S$ and pK_a's of the corresponding conjugate acids (H–A's). A less rigorous treatment in which electrode potentials in S are referred to NHE(aq) using extrathermodynamic quantities is also discussed.

Introduction

The normal hydrogen electrode [NHE(aq)] has long been the standard reference for electrode reactions. The hydronium ion in its standard state, activity of unity in water at 298.15 K, is in equilibrium with dihydrogen gas in its standard state, 1 atm pressure at 298.15 K. The NHE(aq) half-reaction is (1); the

$$H^+_{aq} + e^- \rightleftarrows \tfrac{1}{2}H_2(g) \tag{1}$$
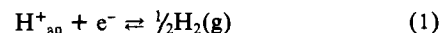
standard free energy change of (1) is taken by convention to equal 0, and hence is assigned an electrode potential of 0. While the